Organic & Biomolecular Chemistry

Cite this: *Org. Biomol. Chem.*, 2012, **10**, 2815

www.rsc.org/obc

PAPER

Helix and hairpin nucleation in short peptides using centrally positioned conformationally constrained dipeptide segments†

Siddappa Chandrappa,[a] Subrayashastry Aravinda,[b] Srinivasarao Raghothama,[c] Rajesh Sonti,[a,c] Rajkishor Rai,[a] Veldore V. Harini,[b] Narayanaswamy Shamala*[b] and Padmanabhan Balaram*[a]

Received 29th October 2011, Accepted 25th January 2012
DOI: 10.1039/c2ob06817f

The effect of incorporation of a centrally positioned Ac_6c-Xxx segment where Xxx = ^{L}Val/^{D}Val into a host oligopeptide composed of L-amino acid residues has been investigated. Studies of four designed octapeptides Boc-Leu-Phe-Val-Ac_6c-Xxx-Leu-Phe-Val-OMe (Xxx = ^{D}Val **1**, ^{L}Val **2**) Boc-Leu-Val-Val-Ac_6c-Xxx-Leu-Val-Val-OMe (Xxx = ^{D}Val **3**, ^{L}Val **4**) are reported. Diagnostic nuclear Overhouse effects characteristic of hairpin conformations are observed for Xxx = ^{D}Val peptides (**1** and **3**) while continuous helical conformation characterized by sequential $N_iH \leftrightarrow N_{i+1}H$ NOEs are favored for Xxx = ^{L}Val peptides (**2** and **4**) in methanol solutions. Temperature co-efficient of NH chemical shifts are in agreement with distinctly different conformational preferences upon changing the configuration of the residue at position 5. Crystal structures of peptides **2** and **4** (Xxx = ^{L}Val) establish helical conformations in the solid state, in agreement with the structures deduced from NMR data. The results support the design principle that centrally positioned type I β-turns may be used to nucleate helices in short peptides, while type I′ β-turns can facilitate folding into β-hairpins.

Introduction

The induction of folded structures in short peptides may be achieved by the appropriate placement of conformationally constrained residues in designed sequences.[1] The imposition of restrictions on the conformational choices at specifically positioned residues permits local folding nuclei to be formed, which can then facilitate the stabilization of short elements of regular secondary structures. α,α-Dialkylated residues, most notably the prototype member of this family α-aminoisobutyric acid (Aib), have been extensively used to design peptide helices.[2] D-Proline has emerged as the residue of choice in the creation of β-hairpins, a consequence of the tendency of ^{D}Pro-Xxx sequences to form type I′ or type II′ β-turn conformations.[1c,3] The insertion of D-amino acids into all L-sequences can also promote folding because of the enhanced tendency of L/D or D/L sequences to favor β-turn conformations.[4] The observation that the centrally positioned Aib-^{D}Ala segment facilitates β-hairpin formation in the octapeptide Boc-Leu-Phe-Val-Aib-^{D}Ala-Leu-Phe-Val-OMe,[5] prompted us to investigate the role of segments containing contiguous α,α-dialkylated and D-residues upon incorporation into all L-amino acid sequences. Fig. 1 provides a comparison of three crystallographically characterized peptide conformations. The Aib-^{D}Xxx segment (Xxx = ^{D}Ala, ^{D}Pro) promotes the formation of a type I′ nucleated β-hairpin structure in designed octapeptides.[5,6] However, the Aib-^{D}Val segment is accommodated into a long continuous right-handed helix in a synthetic 19-residue peptide largely composed of L-residues.[7] In this example, the ^{D}Val residue adopts negative ϕ, ψ values in the α_R region of the Ramachandran map. Several earlier studies have indeed established that D-residues can indeed lie in the α_R region of conformational space,[8] even though the α_L-region is energetically more favorable.[9] Inspection of the three structures in Fig. 1 suggests that centrally positioned segments, containing achiral α,α-dialkylated residues and D-residues as guests in an all L-sequences, could lead to either hairpins or helices. In order to assess the conformational influences of these segments we have investigated the following designed octapeptides.

Boc-Leu-Phe-Val-Ac_6c-^{D}Val-Leu-Phe-Val-OMe (**1**)
Boc-Leu-Phe-Val-Ac_6c-Val-Leu-Phe-Val-OMe (**2**)
Boc-Leu-Val-Val-Ac_6c-^{D}Val-Leu-Val-Val-OMe (**3**)
Boc-Leu-Val-Val-Ac_6c-Val-Leu-Val-Val-OMe (**4**)

Two distinct flanking L-peptide segments were chosen Leu-Phe-Val-Xxx-Yyy-Leu-Phe-Val and Leu-Val-Val-Xxx-Yyy-Leu-Val-Val, in order to probe the role of potential aromatic

[a]*Molecular Biophysics Unit, Indian Institute of Science, Bangalore 560 012, India. E-mail: pb@mbu.iisc.ernet.in; Fax: +91-80-23600683; Tel: +91-80-22932337*
[b]*Department of Physics, Indian Institute of Science, Bangalore 560 012, India. E-mail: shamala@physics.iisc.ernet.in; Fax: +91-80-23602602; Tel: +91-80-22932856*
[c]*NMR Research Centre, Institute of Science, Bangalore 560 012, India*

†Electronic supplementary information (ESI) available: Cif files, stereo diagram of molecular conformations and packing figures for the peptides **2** and **4** and NMR spectra for peptides **1** and **2**. CCDC 850190 (**2**) and 850189 (**4**). For ESI and crystallographic data in CIF or other electronic format see DOI: 10.1039/c2ob06817f

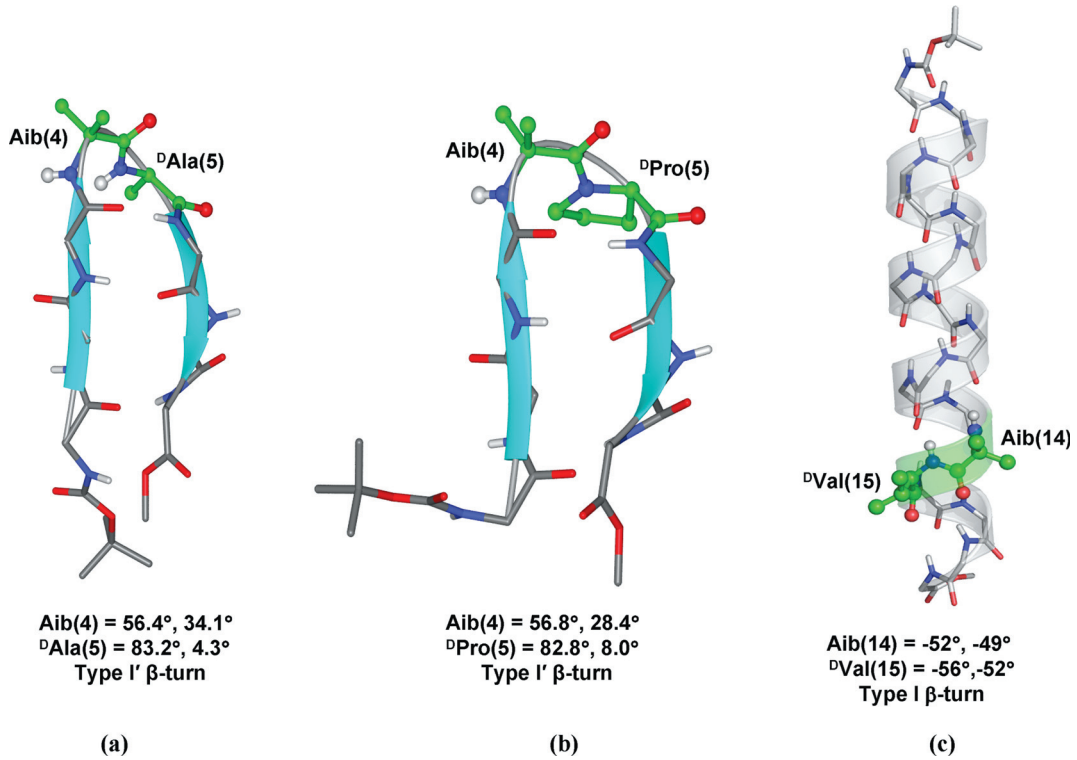

Fig. 1 Aib-^{D}Ala (a) and Aib-^{D}Pro (b) segments adopting type I′ β-turn conformation octapeptide β-hairpins.[5,6] (c) Aib-^{D}Val segment forming a right-handed helical turn (type I β-turn) in a synthetic 19 residue designed peptide.[7] Aib-^{D}Xxx segments are shown as ball and stick.

interactions in stabilizing β-hairpin conformations.[10] The Ac_6c residue (1-aminocyclohexane-1-carboxylic acid)[11] was chosen at position 4, while ^{L}Val and ^{D}Val were placed at position 5, in order to establish the role of residue chirality.

Results and discussion

Fig. 2 compares the aromatic proton and amide NH resonances observed for peptides Boc-Leu-Phe-Val-Ac_6c-^{D}Val-Leu-Phe-Val-OMe (**1**) and Boc-Leu-Phe-Val-Ac_6c-Val-Leu-Phe-Val-OMe (**2**). Clearly distinct distributions of backbone NH chemical shifts are observed for the two peptides. Importantly, the observed upfield shifts of a pair of aromatic protons (Phe(7) $C^{\delta}H$) in peptide **1** (^{D}Val(5)) is characteristic of β-hairpin structures, in which Phe (2) and Phe(7) occur in close proximity at a non-hydrogen bonding site.[10] Amide NH resonances of the peptides in which the aromatic residues have been replaced, **3** and **4**, also shown striking differences with a much larger dispersion in the case of the ^{D}Val peptide **3**. These initial observed differences point to significant change in the conformational propensities of the peptides upon changing the configuration at residue 5. Sequence specific assignment of backbone protons were carried out for all the peptides and vicinal coupling constants and temperature coefficients of chemical shifts for amide NH resonance were determined. The results are summarized in Table 2.

Fig. 3 summarizes the key NOEs observed between the backbone protons in peptide **3** (^{D}Val(5)) and **4** (^{L}Val(5)). In the case of peptide **3** the observation of the NOEs Val(2)$C^{\alpha}H$ ↔ Val(7) $C^{\alpha}H$, Val(3)NH ↔ Leu(6)NH and Leu(1)NH ↔ Val(8)NH are diagnostic of a significant population of β-hairpin conformations

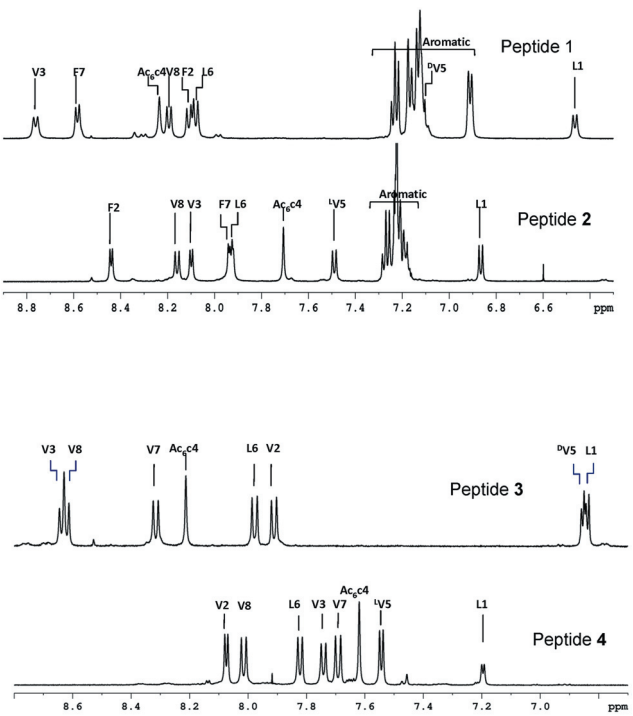

Fig. 2 Low field proton resonance (amide NH aromatic protons) in peptides **1**–**4**. Residue specific assignment are indicated for NH resonances.

in solution. The absence of these sequential NOEs, Val(2)NH ↔ Val(3)NH and Val(3)NH ↔ Ac_6c(4)NH is also suggestive of the fact that helical conformations at the N-terminus are not

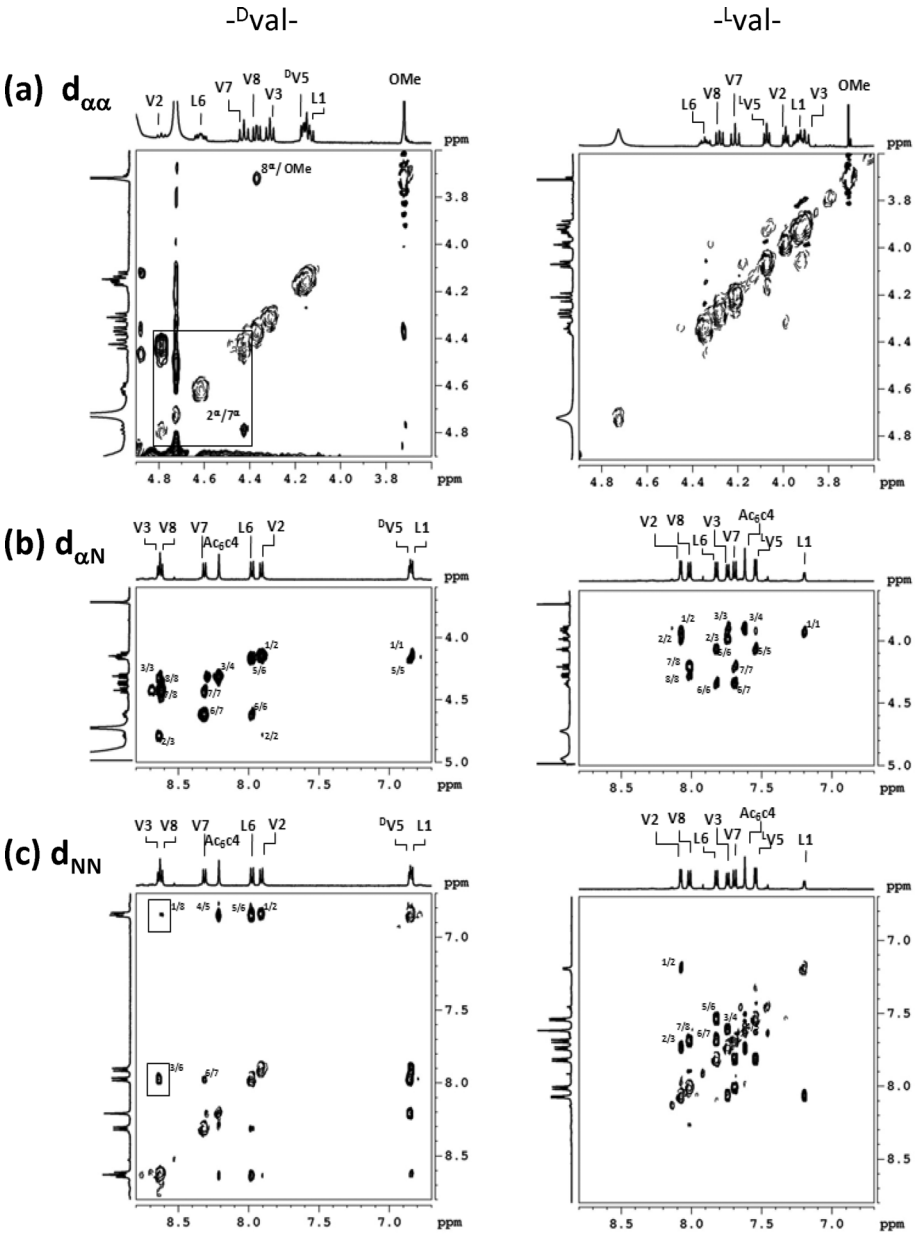

Fig. 3 Partial ROESY spectra of peptides **3** (right) and **4** (left). (a) C^{α} proton region, (b) NH–$C^{\alpha}H$ region, (c) NH–NH region. NOEs characteristic of hairpins ($d_{\alpha\alpha}$ 2/7 and d_{NN} 3/6) are boxed.

populated significantly in solution. In contrast, peptide **4** reveals a complete set of sequential $N_iH \leftrightarrow N_{i+1}H$ NOEs over the entire length of the sequence. Furthermore the diagnostic hairpin NOEs Leu(1)NH ↔ Val(8)NH and Val(2)$C^{\alpha}H$ ↔ Val(7)$C^{\alpha}H$ are also absent. These observations suggest that peptide **3** (^{D}Val(5)) favors β-hairpin conformations in solution, whereas the corresponding ^{L}Val analog (peptide **4**) adopts a continuous helical conformation. Similar results were obtained for peptides **1** and **2**, which contain aromatic residues in the strands at positions 2 and 7. Here again diagnostic hairpin NOEs are observed for (^{D}Val(5)) peptide **1** while peptide **2** (^{L}Val(5)) reveals only NOEs characteristic of a helical conformation (Fig. S1, ESI†).

In the case of ideal β-hairpin conformations, Val(3), Leu(6), Val(8) and Leu(1)NH and CO groups are internally hydrogen bonded. In earlier studies of β-hairpins it has frequently been observed that the Leu(1)NH···Val(8)CO hydrogen bond, which bridges the N and C termini of hairpins, is often frayed.[12] In a 3_{10}-helical structure the NH groups of residues 3 to 8 are expected to be involved in intramolecular 4 → 1(3_{10}) hydrogen bonds, while in an α-helical conformation Val(3)NH may be more solvent exposed. Inspection of the temperature coefficients of chemical shifts (dδ/dT) in methanol provides some useful correlations. The measured dδ/dT values are spread over the range −2.1 to −9.1 ppb K^{-1}. The NH group of residue 2, which is anticipated to be solvent exposed in both helical and hairpin structures, has a dδ/dT value > 6 ppb K^{-1} in all four peptides. The Leu(1)NH group shows significantly lower dδ/dT values (−2.1 ppb K^{-1} and −5.6 ppb K^{-1}) in peptides **1** and **3** (^{D}Val(5)) as compared to peptides **2** and **4** (^{L}Val(5)) (−7.6 ppb K^{-1} and −8.1 ppb K^{-1}). In hairpin structures, where all four possible

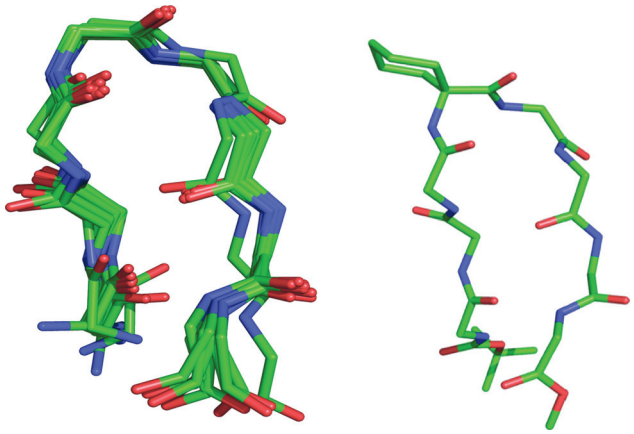

Fig. 4 (Left): Superposition of 10 NMR derived backbone conformations for Boc-Leu-Phe-Val-Ac_6c-^{D}Val-Leu-Phe-Val-OMe (RMSD = 0.39 Å). (Right): One representative hairpin conformation. The Ac_6c residue is shown.

cross-strand hydrogen bonds occur, Leu(1)NH is involved in an interaction with the Val(8)CO group. This hydrogen bond is often disturbed in crystal structures, with Val(8)CO participated in intermolecular interactions. Such fraying is a common feature and is also likely to occur in solution in hydrogen bonding solvents like methanol, which can compete for potential backbone hydrogen bonding sites. The Ac_6c NH (residue 4) might be expected to form an internal hydrogen bond in helical structures, while remaining solvent exposed in the β-hairpin. Indeed, the observed $d\delta/dT$ values for peptides **1** and **3** (−6.4 ppb K^{-1} and −6.1 ppb K^{-1}) are significantly higher than those observed in peptides **2** and **4** (−4.5 ppb K^{-1} and −3.7 ppb K^{-1}). Leu(6)NH exhibits a relatively low $d\delta/dT$ value in all four peptides (−2.2 ppb K^{-1} to −4.3 ppb K^{-1}) consistent with its involvement in an internal hydrogen bond, in both potential hairpin and helical structures. Residue 7NH shows a dramatic difference in $d\delta/dT$ values in peptides **1** and **3** (−7.9 ppb K^{-1} and −8.4 ppb K^{-1}) as compared to peptides **2** and **4** (−3.7 ppb K^{-1} and −3.5 ppb K^{-1}). In hairpins, residue 7NH is solvent exposed, while in helices solvent shielding is anticipated. Val(8)NH shows a relatively high $d\delta/dT$ values in all four peptides (−5.5 ppb K^{-1} to −7.8 ppb K^{-1}). This C-terminus residue is solvent exposed in the octapeptide hairpins, while the C-terminus NH group in short peptide helices is more prone to solvation, resulting in a higher value of the temperature co-efficient. Residue 5NH is expected to be internally hydrogen bonded in helical structures and exhibits moderately low $d\delta/dT$ values (−3.1 ppb K^{-1} and −5.7 ppb K^{-1}), in both peptides **2** and **4**. In the octapeptide hairpin, residue 5NH is a part of the central peptide unit of the nucleating β-turn and does not participate in an internal hydrogen bond. The relatively low $d\delta/dT$ value of −3.1 ppb K^{-1} and −3.7 ppb K^{-1} for residue 5NH is a consequence of steric and electrostatic shielding anticipated in a Type I′ turn, which places the NH group proximate to the Val(3)CO group (N···O ≈ 3.09Å) in peptides **1** and **3**. The observed $d\delta/dT$ value for Val(3)NH are anomalously, high in peptides **1** and **3**, since this NH is expected to be internally hydrogen bonded in the hairpin conformation. Interestingly, Val(3)NH appears at the lowest field position of all NH resonances in β-hairpin peptides containing Leu-Phe-Val/Leu-Val-Val strand segments studied so far. Clearly, factors other than internal hydrogen bonding contribute predominantly to the chemical shift and also its temperature dependence. Interestingly, two distinct side chain conformations have been characterized in crystals for the peptide β-hairpin Boc-Leu-Phe-Val-^{D}Pro-Ala-Leu-Phe-Val-OMe (unpublished results). In one of these conformation the aromatic side chain Phe(2) lies proximate to the Val(3)NH group. The changes in Phe side chain conformation with temperature may contribute significantly to the observed chemical shift of Val(3). Interpretation of temperature co-efficients are often rendered ambiguous because of the difficulties of assigning contributions from competing process like solvation and local conformational changes. Exchange with solvent (CH_3OH) protons at higher temperature also results in broadening of solvent exposed NH resonances. A further point of interest is that the vicinal coupling constant, $^{3}J_{NHC^{\alpha}H}$, values for residues 2, 3 and 6 are significantly greater in peptides **1** and **3** (Xxx = ^{D}Val(5)) as compared to peptides **2** and **4** (5.2 to 7.7 Hz, Xxx = ^{L}Val(5)).

The NMR results thus suggest that the placement of a D-residue at position 5 (peptides **1** and **3**), following an achiral β-turn promoting residue, Ac_6c, results in enhancing the propensity of β-hairpin formation in methanol solution. Solution structures were computed for Boc-Leu-Phe-Val-Ac_6c-^{D}Val-Leu-Phe-Val-OMe (peptide **1**) and Boc-Leu-Val-Val-Ac_6c-^{D}Val-Leu-Val-Val-OMe (peptide **3**) from observed ROESY data. 19 NOEs restraints were used in a simulated annealated protocol resulting in an ensemble of 100 structures. Fig. 4 shows a superposition of 10 β-hairpin structures with an RMSD 0.39 Å for peptide **1**. A single representative conformer illustrating the Ac_6c-^{D}Val hairpin forming turn is also shown. Similar results were also obtained for peptide **3** using measured NOE restraints.

In the case of an L-residue at position 5 (peptides **2** and **4**) the NMR data are consistent with a preponderance of continuous helical conformations. In these cases the helical conformations were established by crystal structure determination as described below.

X-ray diffraction

Fig. 5 shows the molecular conformation of peptides **2** and **4** in crystals. The stereo-view of the molecular conformation is shown in Fig. S2 and S3, ESI.† Peptide **2** crystallized from methanol–water mixture in the orthorhombic space group $P2_12_12_1$, with one molecule in the asymmetric unit. Peptide **4** crystallized from an isopropanol–water mixture in the monoclinic space group $P2_1$, with two peptide molecules and one water molecule in the asymmetric unit. Table 1 summarizes the crystal and diffraction parameters for peptides **2** and **4**. The backbone and side chain torsion angles and the hydrogen bond parameters are summarized in Tables 3 and 4, respectively.

Boc-Leu-Phe-Val-Ac_6c-Val-Leu-Phe-Val-OMe (2). Inspection of ϕ and ψ values from Table 3 reveals that residues 1 to 5 adopt right handed helical conformations and Leu(6) falls in the bridge region of the Ramachandran map. Residues 7 and 8 adopt non-helical values. Val(8) lies in the bridge region. The hydrogen bond pattern reveals that the molecule is stabilized by mixed 4 → 1/5 → 1 hydrogen bonds (three 4 → 1 and three 5 → 1).

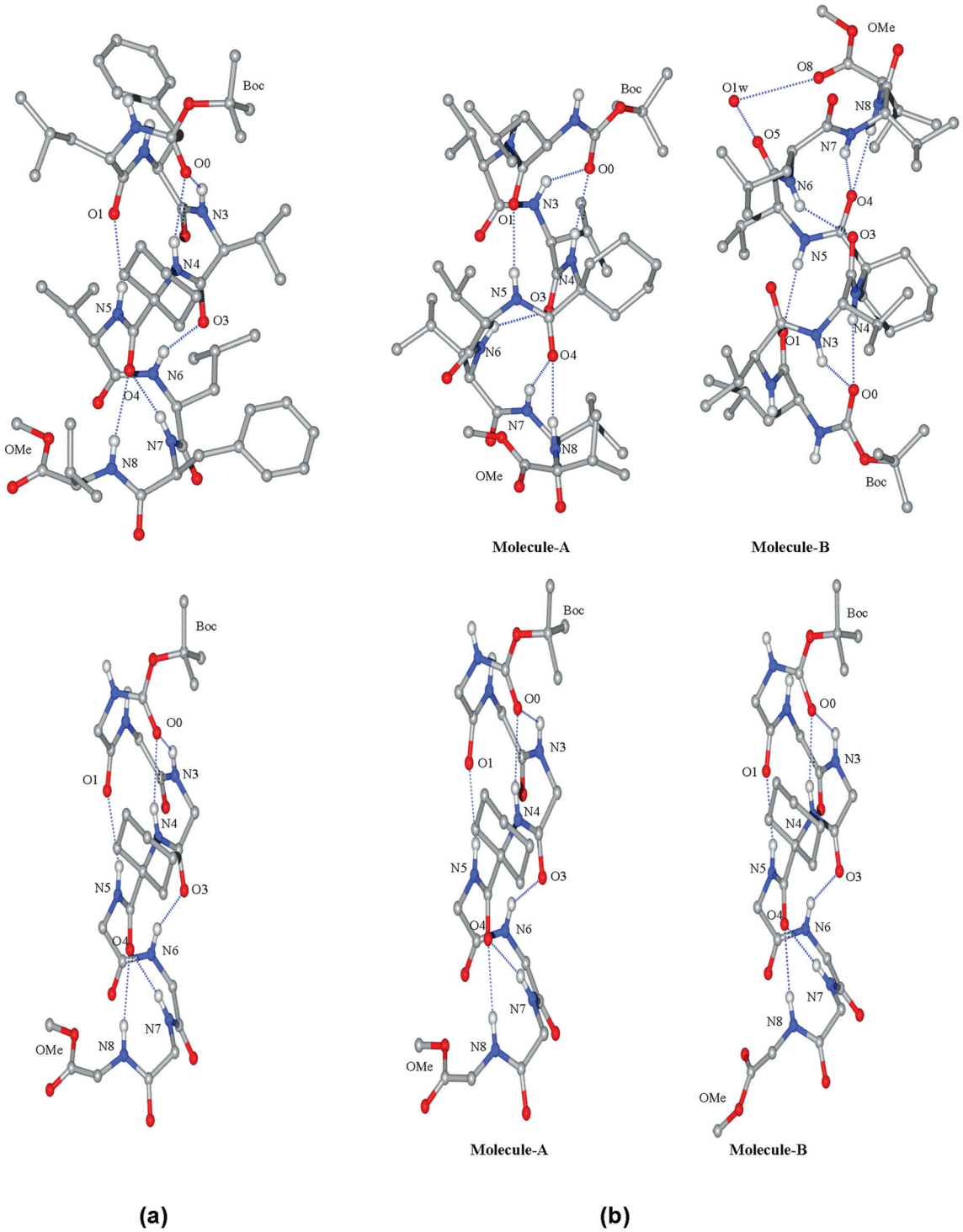

Fig. 5 Top: (a) Molecular conformation of Boc-Leu-Phe-Val-Ac_6c-^{L}Val-Leu-Phe-Val-OMe (**2**) in crystals. (b) The asymmetric unit of peptide Boc-Leu-Val-Val-Ac_6c-^{L}Val-Leu-Val-Val-OMe (**4**) in crystals. Bottom: The backbone of peptides **2** and **4** with only Ac_6c residue shown. The hydrogen bonds are shown as dotted lines.

The simultaneous formation of two hydrogen bonds by a single acceptor CO is observed at the N and C termini. The molecular conformation can be described as a mixed $\alpha/3_{10}$ helix, based on the hydrogen bond pattern. Molecules are packed in crystals as columns of helices, stabilized by two head-to-tail hydrogen bonds. In addition to the head-to-tail hydrogen bonds, aromatic–aromatic interactions between the Phe residues may also contribute (Fig. S4, ESI†). The columns of helices run antiparallel to each other. When viewed down the helix axis, the molecules are arranged in a pseudo-hexagonal grid arrangement[13] (Fig. S5, ESI†). The carbonyl oxygen of Val(2), Val(5) and Val(8) are not involved in hydrogen bond formation.

Table 1 Crystal and diffraction parameter for peptides **2** and **4**

	Peptide **2**	Peptide **4**
Empirical formula	C_{58} H_{90} N_8 O_{11}	C_{50} H_{90} N_8 O_{11}·0.5H_2O
Crystal habit	Transparent	Transparent, needle like
Crystal size (mm)	0.8 × 0.3 × 0.2	0.5 × 0.15 × 0.15
Crystallizing solvent	Methanol–water	Isopropanol–water
Space group	$P2_12_12_1$	$P2_1$
Cell parameters		
a (Å)	11.312(4)	10.516(3)
b (Å)	19.868(6)	27.593(4)
c (Å)	28.099(9)	21.050(3)
α (°)	90	90
β (°)	90	97.919(3)
γ (°)	90	90
Volume (Å^3)	6315(3)	6050(2)
Z	4	4
Molecules/asym.unit	1	2
Cocrystallized solvent	None	One water molecule
Molecular weight	1075.38	978.3 + 9 = 987.3
Density (g cm^{-3}) (cal)	1.131	1.084
F (000)	2328	2152
Radiation	MoK$_\alpha$ (λ = 0.71073 Å)	MoK$_\alpha$ (λ = 0.71073 Å)
Temperature (°C)	21	21
2θ max (°)	53.8	56.1
Scan type	ω	ω
Measured reflections	62 458	71 594
Independent reflections	12 729	28 276
Unique reflections	7153	14 733
Observed reflections [$\|F\| > 4\sigma(F)$]	4488	8010
Final R(%)	7.67	6.44
Final wR_2(%)	16.19	15.73
Goodness-of-fit (S)	1.075	0.98
$\Delta\rho_{max}$ (e Å^{-3})	0.39	0.63
$\Delta\rho_{min}$ (e Å^{-3})	−0.24	−0.24
No. of restraints/parameters	0/694	3/1252
Data-to-parameter ratio	6.5 : 1	6.4 : 1

Boc-Leu-Val-Val-Ac$_6$c-Val-Leu-Val-Val-OMe (4). Inspection of ϕ, ψ values from Table 3 reveals that residues 1 to 5 adopt right handed helical conformations and Leu(6) falls in the bridge region, in both the molecules A and B. Residues 7 and 8 adopt non-helical values. In molecule A Val(8) lies in the bridge region and in the extended region in molecule B. The hydrogen bond pattern reveals that the molecule is stabilized by mixed 4 → 1/5 → 1 hydrogen bonds (three 4 → 1 and three 5 → 1). Acceptors at the N and C termini form two simultaneous interactions with the donor NH groups. The molecular conformation can be described as a mixed α/3_{10} helix, based on the hydrogen bond pattern. In molecule B, there are additional hydrogen bonds observed between water (O1w) and Val(5)CO and Val(8)CO. An interesting feature in the present crystal structure is the coexistence of solvated and unsolvated molecules in the asymmetric unit. The molecules are arranged antiparallel to each other (interhelical angle ~ 176.5°) and packed as column of helices stabilized by two head-to-tail hydrogen bonds. The columns of helices run antiparallel in pairs in the crystal lattice. When viewed down the helix axis, the molecules are arranged in a square grid arrangement (Fig. S6, ESI†). In molecule A, the carbonyl oxygen atoms of Val(2), Val(5) and Val(8) are not involved in any hydrogen bond formation and in molecule B the carbonyl

Table 2 NMR parameters for peptides **1** to **4** in CD_3OH

	Peptide **1**				Peptide **2**				Peptide **3**				Peptide **4**			
Turn segment	Ac$_6$c-^{D}Val				Ac$_6$c-^{L}Val				Ac$_6$c-^{D}Val				Ac$_6$c-^{L}Val			
Residues	δNH (ppm)	δC$^\alpha$H	$^3J_{NHC^\alpha H}$ (Hz)	dδ/dT (ppb K^{-1})	δNH (ppm)	δC$^\alpha$H	$^3J_{NHC^\alpha H}$ (Hz)	dδ/dT (ppb K^{-1})	δNH (ppm)	δC$^\alpha$H	$^3J_{NHC^\alpha H}$ (Hz)	dδ/dT (ppb K^{-1})	δNH (ppm)	δC$^\alpha$H	$^3J_{NHC^\alpha H}$ (Hz)	dδ/dT (ppb K^{-1})
Leu(1)	6.47	4.08	7.9	−2.1	6.86	4.03	7.5	−7.6	6.83	4.15	8.3	−5.6	7.20	3.95	4.3	−8.1
Phe(2)/Val(2)	8.10	5.26	9.0	−6.1	8.44	4.39	5.2	−7.7	7.92	4.79	9.3	−6.0	8.07	3.99	5.2	−9.7
Val (3)	8.75	4.31	8.3	−9.1	8.09	3.83	6.1	−6.3	8.64	4.30	8.1	−6.5	7.74	3.91	7.7	−2.8
Ac$_6$c (4)	8.33	—	—	−6.4	7.70	—	—	−4.5	8.22	—	—	−6.1	7.62	—	—	−3.7
^{D}Val(5)/^{L}Val(5)	7.12	4.11	7.2	−3.1	7.49	4.12	7.7	−3.1	6.86	4.19	7.8	−3.7	7.54	4.07	6.0	−5.7
Leu (6)	8.08	4.64	8.9	−4.3	7.93	4.32	7.3	−3.7	7.98	4.62	8.8	−3.3	7.82	4.35	7.5	−2.2
Phe(7)/Val(7)	8.58	4.67	7.6	−7.9	7.92	4.72	8.4	−3.7	8.32	4.43	8.7	−8.4	7.69	4.21	8.9	−3.5
Val(8)	8.19	4.16	8.9	−5.9	8.15	4.28	8.4	−7.8	8.63	4.37	8.5	−7.1	8.01	4.28	8.3	−5.5

Table 3 Torsion angles for peptides **2** and **4** (°)[a]

Residue	Peptide 2 (Xxx = Phe)			Peptide **4** (Xxx = Val)					
				Molecule-A			Molecule-B		
	ϕ	ψ	ω	ϕ	ψ	ω	ϕ	ψ	ω
Leu(1)	−60.0[b]	−29.2	178.5	−45.9[b]	−45.6	−175.8	−51.3[e]	−41.1	−177.2
Xxx(2)	−59.7	−30.2	174.5	−58.1	−40.4	174.7	−59.2	−38.7	175.3
Val(3)	−87.9	−42.4	−176.7	−70.1	−47.6	−174.3	−69.9	−45.7	−175.4
Ac_6c(4)	−51.4	−41.2	−174.1	−50.0	−48.4	−171.1	−51.7	−47.7	−172.8
Val(5)	−70.4	−10.4	173.2	−74.8	−12.2	172.5	−75.0	−11.2	172.9
Leu(6)	−82.9	−12.2	−176.1	−91.2	−4.7	−179.6	−93.2	0.5	−178.3
Xxx(7)	−110.1	−47.4	−176.5	−108.7	−46.2	−177.6	−113.7	−52.9	−174.4
Val(8)	−124.6	−16.9[c]	−178.7[d]	−119.3	−11.5[c]	177.6[d]	−96.7	154.0[f]	178.6[g]
Side chain	χ^1	χ^2		χ^1	χ^2		χ^1	χ^2	
Leu(1)	−74.4	−76.3, 155.1		−175.0	76.0, −163.8		−178.8	−92.6, 153.9	
Xxx(2)	−79.3	22.2, −158.1		−68.0, 167.4			−68.7, 172.6		
Val(3)	−61.8, 175.0			−61.1, 174.3			−62.5, 173.0		
Val(5)	−68.5, 69.0			−61.3, 65.9			−60.7, 68.5		
Leu(6)	−54.5	−54.6, 177.3		−67.3	−69.1, 168.0		−70.0	−69.8, 167.5	
Xxx(7)	−69.9	79.2, −98.8		−60.2, 176.9			−61.2, 175.2		
Val(8)	−67.6, 60.1			−64.1, 60.3			−64.2, 61.8		

[a] The torsion angles for rotation about bonds of the peptide backbone (ϕ, ψ and ω) and about bonds of the amino acid side chains (χ^1, χ^2) as suggested by the IUPAC-IUB Commission on Biochemical Nomenclature. *Biochemistry* 1970, **9**, 3471–3479. The standard deviation in torsion angles are 0.3° and 0.2° for peptides **2** and **4** respectively. [b] C′(0)–N(1)–C^{α}(1)–C′(1). [c] N(8)–C^{α}(8)–C′(8)–O1(OMe). [d] C^{α}(8)–C′(8)–O1(OMe)–C1(OMe). [e] C′(10)–N(11)–C^{α}(11)–C′(11). [f] N(18)–C^{α}(18)–C′(18)–O2(OMe). [g] C^{α}(18)–C′(18)–O2(OMe)–C2(OMe).

oxygen of Val(2) is not involved in hydrogen bond formation. In both peptides **2** and **4** the amino group of Ac_6c is in an axial position on the cyclohexane ring. The molecular conformations established for peptide **2** and **4** in crystals are in agreement with the helical conformations deduced from NMR data in the previous section. Repeated attempts to obtain crystals of peptides **1** and **3** over several years were unsuccessful.

Conclusion

The incorporation of sterically constrained α,α-dialkylated residues at central positions in short sequences containing L-amino acids induces *right-handed* helix formation. Several crystal structures are now available for short sequences containing a single α,α-dialkylated residue, in which helical folds, closely related to right-handed 3_{10}/α-helical structures, have been characterized.[1,2] Helix nucleation may be favored by the tendency of the central segment containing α,α-dialkylated residue to form type I/III β-turn conformations.[2e] The present study was designed in order to explore the effect of changing the conformation of the chiral residue that immediately follows the stereochemically constrained residue. This comparative study of octapeptides containing centrally positioned Ac_6c-^{L}Val and Ac_6c-^{D}Val segments reveals that helices are predominately populated in solution in the former, while β-hairpins predominate in the latter. Secondary structure nucleation by designed segments with limited conformational choices can prove effective in the design of short peptides adopting well defined conformations. In many previous studies of peptide β-hairpins the D-proline residue has been used to promote formation of type II′ β-turns as a means of hairpin nucleation.[3,14] The present study provides further support for the design principle that type I′ turns constructed using α,α-dialkylated residues are also effective in hairpin nucleation.[5,6]

Experimental section

Peptide synthesis

The peptides were synthesized by standard solution-phase procedures. The *tert*-butoxycarbonyl (Boc) group was used for N-terminus protection, and the C-terminus was protected as a methyl ester. Deprotections were performed using 98% formic acid for the Boc group and saponification for the methyl ester. The final step in the synthesis of peptides was achieved by the fragment condensation of Boc-Leu-Val-Val-OH/Boc-Leu-Phe-Val-OH with H_2N-Ac_6c-X-Leu-Val-Val-OMe/H_2N-Ac_6c-X-Leu-Phe-Val-OMe (X = L-Val or D-Val), using *N*,*N*′-dicyclohexylcarbodiimide (DCC)–1-hydroxybenzotriazole (HOBt) as the coupling reagent. All the intermediates were characterized by electrospray ionization mass spectrometry (ESI-MS) on a Bruker Daltonics Esquire-3000 instrument and thin-layer chromatography (TLC) on silica gel and used without further purification for the final step. The target peptides were purified by reverse-phase medium-pressure liquid chromatography (RP-MPLC, C_{18}, 40–60 μm) and high-performance liquid chromatography (HPLC) on a reverse-phase C_{18} column (5–10 μm, 7.8 mm × 250 mm) using methanol–water gradients. The purified peptides were characterized by ESI-MS. Mass spectral data (*m*/*z*): peptides **1** and **2**, 1074.2 $[M + H]^+$ (M_{cal}) 1073.4 Da, 1097.1 $[M + Na]^+$, 1113.2 $[M + K]^+$; **3** and **4**, 978.1 $[M + H]^+$ (M_{cal}) 977.4 Da, 1001.2 $[M + Na]^+$, 1017.4 $[M + K]^+$.

NMR spectroscopy

Experiments were carried out on Bruker AV700 and DRX500 spectrometers. 1D and 2D spectra were recorded at a peptide concentration of ~5 mM in CD_3OH at 300 K. Resonance

Table 4 Hydrogen bonds in peptides **2** and **4**

Type	Donor	Acceptor	N···O/O···O (Å)	H···O (Å)	C═O···H (°)	C═O···N (°)	O···H–N (°)
Peptide 2							
Intermolecular							
	N(1)	O(6)[a]	2.870	2.055	130.4	134.7	157.8
	N(2)	O(7)[a]	3.168	2.336	137.7	141.8	163.0
Intramolecular							
4 → 1	N(3)	O(0)	2.923	2.199	121.9	129.8	141.7
5 → 1	N(4)	O(0)	3.074	2.237	144.7	149.1	164.2
5 → 1	N(5)	O(1)	3.132	2.306	149.8	151.4	161.2
4 → 1	N(6)	O(3)	2.899	2.100	119.6	126.9	154.2
4 → 1	N(7)	O(4)	2.985	2.162	117.7	122.9	160.1
5 → 1	N(8)	O(4)	3.120	2.265	169.5	171.3	172.5
Peptide 4							
Molecule-A							
Intermolecular							
	N(11)	O(16)[b]	2.908	2.093	126.6	130.7	158.0
	N(12)	O(17)[b]	3.024	2.167	151.8	153.0	173.8
Intramolecular							
4 → 1	N(13)	O(10)	2.914	2.343	125.8	136.3	124.2
5 → 1	N(14)	O(10)	3.032	2.184	149.0	152.1	168.4
5 → 1	N(15)	O(11)	3.047	2.210	159.5	160.4	164.2
4 → 1	N(16)	O(13)	2.899	2.100	119.6	126.9	154.2
4 → 1	N(17)	O(14)	2.985	2.162	117.7	122.9	160.1
5 → 1	N(18)	O(14)	3.006	2.150	169.3	170.4	173.3
Molecule-B							
Intermolecular							
	N(21)	O(26)[c]	2.869	2.065	124.0	129.2	155.5
	N(22)	O(27)[c]	3.103	2.251	147.1	149.0	171.1
Solvent	O1w	O(25)	2.756				
Solvent	O1w	O(28)	3.222				
Intramolecular							
4 → 1	N(23)	O(20)	2.926	2.343	123.5	133.7	125.4
5 → 1	N(24)	O(20)	3.074	2.237	144.7	149.1	164.2
5 → 1	N(25)	O(21)	3.132	2.306	149.8	151.4	161.2
4 → 1	N(26)	O(23)	2.992	2.267	111.3	121.2	142.1
4 → 1	N(27)	O(24)	3.057	2.241	112.1	116.1	158.4
5 → 1	N(28)	O(24)	3.111	2.254	173.6	172.2	174.2

[a] Symmetry related by $-x+3/2$, $-y$, $z-1/2$. [b] Symmetry related by $-x+1$, $y-1/2$, $-z+1$. [c] Symmetry related by $-x+1$, $y+1/2$, $-z$. The standard deviation in bond lengths and bond angles are 0.004 Å and 0.3° and 0.002 Å and 0.2° for peptides **2** and **4** respectively.

assignments were carried out with the help of 1D and 2D spectra. Residue specific assignments were obtained from TOCSY experiments, whereas ROESY spectra permitted sequence specific assignments. The TPPI (time proportional phase incrementation) method was used for phase sensitive 2D experiments. A data set of 1024 × 450 was used for acquiring the data. The same data set was zero filled to yield a data matrix of size 2048 × 1024, before Fourier transformation. A spectral width of 6000 and 8700 Hz was used in both dimensions at 500 and 700 MHz, respectively. Mixing times of 100 and 200 ms were used for TOCSY and ROESY, respectively. Shifted square sine bell windows were used and all processing was done using BRUKER TOPSPIN software.

Structure calculations

Solution structures were computed using the Discover module (version 2000) of InsightII (Accelyrs, San Diego, CA) from ROESY cross-peaks. The NOE restraints were categorized into three groups: strong (2.5 Å upper limit), medium (3.5 Å upper limit), and weak (5.0 Å upper limit). These distances were employed using generic distance restraints with force constants of 1 kcal mol^{-1} $Å_2^{-1}$ and a maximum force value of 1000 kcal mol^{-1} $Å_2^{-1}$. The consistent valence force field (CVFF) was applied for all calculations. Prior to every restrained dynamics simulation the system was equilibrated for 1 ps. The energy minimized structures were subjected to constrained MD simulations for a duration of 2 ns (8 cycles each of 2.5 ps period, of the Simulated Annealing Protocol). After simulating for 2.5 ps at high temperature, the system temperature was reduced exponentially over a 2.5 ps period to reach a final temperature of 300 K. At regular intervals, 100 conformers were extracted, leading to an ensemble of 100 structures and subjected to energy minimization by conjugate gradient method. The resulting structures were analyzed with Pymol and InsightII. A total of 19 NOE restraints were used for both peptides **1** and **3**.

X-ray diffraction

Single crystals of peptides **2** and **4** were grown from methanol–water and isopropanol–water solutions, respectively. Despite repeated trials, suitable crystals of peptides **1** and **3** could not be obtained. Table 1 summarizes the crystallographic data and other details for the compounds **2** and **4**. X-ray diffraction data were collected on a Bruker AXS SMART APEX CCD diffractometer using MoK_{α} radiation (λ = 0.71073 Å). The structures were solved by direct methods using SHELXD.[15] For peptide **2**, a fragment containing 69 atoms was obtained. For peptide **4** two fragments were obtained containing 59 and 47 atoms. The remaining atoms and solvent molecules were located from difference Fourier-maps. Full matrix least squares refinement was carried out using SHELXL-97.[15] The hydrogen atoms were fixed geometrically in idealized positions and refined in the final cycle of refinement, as riding over the atoms to which they are bonded. The final *R*-factor was 7.67% for peptide **3** and 6.44% for peptide **4**. The crystallographic coordinates for the structures are deposited at the Cambridge Crystallographic Data Centre with CCDC numbers 850190 (**2**) and 850189 (**4**).

Acknowledgements

This research was supported by a grant from the Council of Scientific and Industrial Research (CSIR) and a program grant from the Department of Biotechnology, India, in the area of Molecular Diversity and Design, India. S. C. is supported by the award of a UGC-DSK Postdoctoral Fellowship from the University Grants Commission (UGC), India. S. A. and V. V. H. thank the CSIR for a Research Associateship and a Senior Research Fellowship.

References

1 (*a*) R. Kaul and P. Balaram, *Bioorg. Med. Chem.*, 1999, **7**, 105; (*b*) P. Balaram, *J. Pept. Res.*, 1999, **54**, 195; (*c*) J. Venkatraman, S. C. Shankaramma and P. Balaram, *Chem. Rev.*, 2001, **101**, 3131; (*d*) S. Aravinda, N. Shamala, R. S. Roy and P. Balaram, *Proc.–Indian Acad. Sci., Chem. Sci.*, 2003, **115**, 373.

2 (*a*) G. R. Marshall and H. E. Bosshard, *Circ. Res.*, 1972, **31**, 143; (*b*) N. Shamala, R. Nagaraj and P. Balaram, *Biochem. Biophys. Res. Commun.*, 1977, **79**, 292; (*c*) N. Shamala, R. Nagaraj and P. Balaram, *J. Chem. Soc., Chem. Commun.*, 1978, 996; (*d*) R. Nagaraj, N. Shamala and P. Balaram, *J. Am. Chem. Soc.*, 1979, **101**, 16; (*e*) B. V. V. Prasad and P. Balaram, *Crit. Rev. Biochem. Mol. Biol.*, 1984, **16**, 307; (*f*) C. Toniolo and E. Benedetti, *ISI Atlas Sci. Biochem.*, 1988, **1**, 225; (*g*) I. L. Karle and P. Balaram, *Biochemistry*, 1990, **29**, 6747; (*h*) C. Toniolo and E. Benedetti, *Trends Biochem. Sci.*, 1991, **16**, 350; (*i*) C. Toniolo and E. Benedetti, *Macromolecules*, 1991, **24**, 4004; (*j*) E. Benedetti, *Biopolymers*, 1996, **40**, 3; (*k*) I. L. Karle, *Biopolymers*, 1996, **40**, 157; (*l*) C. Toniolo, M. Crisma, F. Formaggio and C. Peggion, *Biopolymers*, 2001, **60**, 396; (*m*) C. Toniolo, M. Crisma, F. Formaggio, C. Peggion, Q. B. Broxterman and B. Kaptein, *Biopolymers*, 2004, **76**, 162; (*n*) M. Crisma, F. Formaggio, A. Moretto and C. Toniolo, *Biopolymers*, 2006, **84**, 3.

3 (*a*) S. K. Awasthi, S. Raghothama and P. Balaram, *Biochem. Biophys. Res. Commun.*, 1995, **216**, 375; (*b*) I. L. Karle, S. K. Awasthi and P. Balaram, *Proc. Natl. Acad. Sci. U. S. A.*, 1996, **93**, 8189; (*c*) T. S. Haque, J. C. Little and S. H. Gellman, *J. Am. Chem. Soc.*, 1996, **118**, 6975.

4 R. Chandrasekaran, A. V. Lakshminarayanan, U. V. Pandya and G. N. Ramachandran, *Biochim. Biophys. Acta*, 1973, **303**, 14.

5 S. Aravinda, N. Shamala, R. Rai, H. N. Gopi and P. Balaram, *Angew. Chem., Int. Ed.*, 2002, **41**, 3863.

6 U. S. Raghavender, S. Aravinda, R. Rai, N. Shamala and P. Balaram, *Org. Biomol. Chem.*, 2010, **8**, 3133.

7 I. L. Karle, H. N. Gopi and P. Balaram, *Proc. Natl. Acad. Sci. U. S. A.*, 2003, **100**, 13946.

8 S. Aravinda, N. Shamala, S. Desiraju and P. Balaram, *Chem. Commun.*, 2002, 2454.

9 (*a*) R. Fairman, S. J. Anthony-Cahill and W. F. DeGrado, *J. Am. Chem. Soc.*, 1992, **114**, 5458; (*b*) Y. Chen, C. T. Mant and R. S. Hodges, *J. Pept. Res.*, 2002, **59**, 18.

10 (*a*) C. Zhao, P. L. Polavarapu, C. Das and P. Balaram, *J. Am. Chem. Soc.*, 2000, **122**, 8228; (*b*) C. Das, G. A. Naganagowda, I. L. Karle and P. Balaram, *Biopolymers*, 2001, **58**, 335; (*c*) A. Rajagopal, S. Aravinda, S. Raghothama, N. Shamala and P. Balaram, *Biopolymers (Pept. Sci.)*, 2011, DOI: 10.1002/bip.22003.

11 (*a*) R. Bardi, A. M. Piazzesi, C. Toniolo, M. Sukumar, P. Antony Raj and P. Balaram, *Int. J. Pept. Protein Res.*, 1985, **25**, 628; (*b*) P. K. C. Paul, M. Sukumar, R. Bardi, A. M. Piazzesi, G. Valle, C. Toniolo and P. Balaram, *J. Am. Chem. Soc.*, 1986, **108**, 6363; (*c*) G. Valle, M. Crisma, C. Toniolo, N. Sen, M. Sukumar and P. Balaram, *J. Chem. Soc., Perkin Trans. 2*, 1987, 393; (*d*) A. Crisma, M. Bonora, G. M. Sonara and C. Toniolo, *Macromolecules*, 1988, **21**, 2064.

12 (*a*) S. Aravinda, V. V. Harini, N. Shamala, C. Das and P. Balaram, *Biochemistry*, 2004, **43**, 1832; (*b*) V. V. Harini, S. Aravinda, R. Rai, N. Shamala and P. Balaram, *Chem.–Eur. J.*, 2005, **11**, 3609; (*c*) Kantharaju, S. Raghothama, U. S. Raghavender, S. Aravinda, N. Shamala and P. Balaram, *Biopolymers*, 2009, **92**, 405.

13 (*a*) I. L. Karle, *Acta Crystallogr., Sect. B: Struct. Sci.*, 1992, **48**, 341; (*b*) I. L. Karle, *Acc. Chem. Res.*, 1999, **32**, 693.

14 (*a*) C. Das, S. Raghothama and P. Balaram, *J. Am. Chem. Soc.*, 1998, **120**, 5812; (*b*) J. Venkatraman, G. A. Naganagowda and P. Balaram, *J. Am. Chem. Soc.*, 2002, **124**, 4987; (*c*) I. L. Karle, H. N. Gopi and P. Balaram, *Proc. Natl. Acad. Sci. U. S. A.*, 2002, **99**, 5160; (*d*) H. N. Gopi, R. S. Roy, S. Raghothama, I. L. Karle and P. Balaram, *Helv. Chim. Acta*, 2002, **85**, 3313; (*e*) R. S. Roy, H. N. Gopi, S. Raghothama, R. D. Gilardi, I. L. Karle and P. Balaram, *Biopolymers*, 2005, **80**, 787; (*f*) R. S. Roy, H. N. Gopi, S. Raghothama, I. L. Karle and P. Balaram, *Chem.–Eur. J.*, 2006, **12**, 3295; (*g*) R. Rai, P. G. Vasudev, K. Ananda, S. Raghothama, N. Shamala, I. L. Karle and P. Balaram, *Chem.–Eur. J.*, 2007, **13**, 5917; (*h*) S. Chatterjee, P. G. Vasudev, S. Raghothama, C. Ramakrishnan, N. Shamala and P. Balaram, *J. Am. Chem. Soc.*, 2009, **131**, 5956.

15 G. M. Sheldrick, *Acta Crystallogr., Sect. A: Found. Crystallogr.*, 2008, **64**, 112.